Sustainable Energy & Fuels

Effective Strategy for Enhancing Z-scheme Water Splitting with IO_3^-/I^- Redox Mediator by using Visible Light Responsive TaON Photocatalyst Co-loaded with Independently Optimized Two Different Cocatalysts

Journal:	*Sustainable Energy & Fuels*
Manuscript ID	SE-ART-03-2019-000136.R1
Article Type:	Paper
Date Submitted by the Author:	04-Apr-2019
Complete List of Authors:	Iwase, Yukari; Graduate School of Engineering, Kyoto University Tomita, Osamu; Graduate School of Engineering, Kyoto University Higashi, Masanobu; Graduate School of Engineering, Kyoto University Nakada, Akinobu; Graduate School of Engineering, Kyoto University Abe, Ryu; Graduate School of Engineering, Kyoto University

SCHOLARONE™
Manuscripts

ARTICLE

Effective Strategy for Enhancing Z-scheme Water Splitting with IO₃⁻/I⁻ Redox Mediator by using Visible Light Responsive TaON Photocatalyst Co-loaded with Independently Optimized Two Different Cocatalysts

Yukari Iwase,[a] Osamu Tomita,[a] Masanobu Higashi,[a] Akinobu Nakada[a] and Ryu Abe[*a, b]

Loading an efficient cocatalyst that can selectively enhance favorable reactions is an effective way to improve the efficiency of Z-scheme water splitting with a redox mediator such as IO_3^-/I^-. Given a recent finding on a highly active $Ru(OH)_xCl_y$ cocatalyst for IO_3^- reduction on TaON photocatalyst, here we systematically investigate Rh, Co, and Ir-based cocatalyst for enhancing water oxidation and thereby improving the total efficiency of O_2 evolution on TaON with the help of the $Ru(OH)_xCl_y$ cocatalyst. The calcination temperature of metal cation (i.e., Rh, Co or Ir) species on TaON, which is co-loaded by $Ru(OH)_xCl_y$ species at a fixed temperature of 200 °C, significantly affected the rate of O_2 evolution from aqueous solution containing IO_3^- under visible light irradiation. The rate of O_2 evolution was basically increased with the increased temperature at the cocatalyst loading up to 400 °C (for Ir) and 500 °C (for Rh and Co), while the calcination at 600 °C drastically lowered the activity due to detrimental effect on the TaON itself. The highest O_2 evolution rate was obtained by the loading of Rh species at 500 °C, followed by co-loading of $Ru(OH)_xCl_y$ at 200 °C, on TaON. The results of both photocatalytic reactions and electrochemical measurements revealed that the Rh species loaded at 500 °C, which mainly consist of Rh oxides, promote the water oxidation more effectively than conventional CoO_x or IrO_x species. The rates of H_2 and O_2 evolution in an overall water splitting via Z-scheme mechanism were significantly increased by use of the TaON photocatalyst co-loaded with Rh and Ru species as the O_2-evolving photocatalyst, in place of the TaON loaded with only conventional RuO_2 species or previously reported TaON co-loaded with $Ru(OH)_xCl_y$ and Co-based species. These results indicate the effectiveness of co-loading of cocatalysts that are independently-optimized for water oxidation and IO_3^- reduction for improving the efficiency of Z-scheme water splitting.

Introduction

Photocatalytic water splitting using semiconductor materials has attracted much attention because of its potential for a clean and sustainable H_2 production from abundant water by harvesting solar light energy.[1-6] To achieve practically high H_2 production efficiency under natural sunlight on the Earth's surface, a considerable fraction of photons in visible light region must be utilized effectively. In this regard, various photocatalyst materials with narrower bandgaps than 3.0 eV, including metal oxides, (oxy)nitrides, (oxy)sulfides, and (oxy)halides, have been so far developed.[5-7] However, the number of successful reports on overall water splitting (i.e., simultaneous generation of H_2 and O_2 with stoichiometric ratio) using single photocatalyst material is still limited because the material must simultaneously have a narrow band gap with suitable

conduction and valence band edges for H_2 and O_2 generation, and stability under photoirradiation. Two-step (i.e., the Z-scheme) water splitting system, which basically consists of two different photocatalysts (one for H_2 evolution and the another for O_2-evolution), has then been emerged as one of the promising strategies for harvesting a wider range of visible light since the energy required to drive each photocatalysis process can be reduced.[4-10] The majority of such Z-scheme water splitting systems employs a redox mediator that dissolves in the aqueous solution and plays a decisive role in transporting electrons from the O_2-evolving photocatalyst to the H_2-evolving one.[4-13] The redox cycle between iodate (IO_3^-) and iodide (I^-) is widely employed in the Z-scheme water splitting systems, in which various semiconductor materials, including metal oxides, oxynitrides, oxysulfides, and carbon nitrides, have been used probably due to the fact that the redox cycle of IO_3^-/I^- can proceed under wider pH range (pH 6-11) compared to that of Fe^{3+}/Fe^{2+} couple (pH < 2.5).[4-10] For example, some oxynitrides and nitrides (e.g., TaON and Ta_3N_5)[14-18] have been successfully employed as both H_2- and O_2-evolving photocatalysts with the help of IO_3^-/I^- redox mediator.[10, 19-21] However, the multielectron redox nature ($IO_3^- + 6e^- + 3H_2O \longrightarrow I^- + 6OH^-$) is

undoubtedly a disadvantage and actually necessitates the loading of an effective cocatalyst (e.g., PtO_x and RuO_2) to accelerate the six-electron process.[19, 20, 22, 23]

We have recently reported that the $Ru(OH)_xCl_y$ species loaded onto an oxynitride TaON, which is known as one of the promising visible light responsive photocatalyst, by the impregnation of aqueous $RuCl_3 \bullet nH_2O$ followed by calcination at relatively low temperature (at or below 200 °C) function as highly active cocatalyst for IO_3^- reduction.[24] The activity of $Ru(OH)_xCl_y$ species were revealed to be superior to the previously-reported RuO_2 cocatalyst[19, 20] loaded at relatively high temperature (at or above 300 °C). We also found that co-loading of this $Ru(OH)_xCl_y$ cocatalyst with Co-based cocatalyst (e.g., $Co(OH)_2$) that can promote water oxidation is quite effective to increase the rate of O_2 evolution on TaON photocatalyst in the presence of IO_3^-, indicating the great possibility of co-loading of two different cocatalysts that are independently-optimized for each reaction (reduction and oxidation) to construct the efficient Z-scheme water splitting system in the presence of redox mediator such as IO_3^-/I^-.

In this study, we thus attempted to further improve the photocatalytic activity of TaON by optimizing the cocatalyst for water oxidation, including Rh and Ir-based ones loaded at varied calcination temperatures along with Co-based one, with the help of $Ru(OH)_xCl_y$ cocatalyst for IO_3^- reduction.

Experimental

Preparation of co-catalyst loaded TaON particles

The particulate sample of TaON was prepared according to a previously reported method.[14] Briefly, commercially available Ta_2O_5 particles (99.99%, Kojundo Chemical Co., Ltd) were heated under a stream of NH_3 gas (99.99%, 60 mL min^{-1}) at 850 °C for 24 h. Loading of Rh, Co or Ir species onto TaON particles was performed by an impregnation method from aqueous solutions containing each cation precursor; sodium hexachlororhodate(III) n-hydrate ($Na_3[RhCl_6] \bullet nH_2O$, 80%, Kanto Chemical Co., Inc.), cobalt(II) nitrate hexahydrate ($Co(NO_3)_2 \bullet 6H_2O$, 98.0%, Wako Pure Chemical Industries, Ltd.) or sodium hexachloroiridate(IV) hexahydrate ($Na_4[IrCl_6] \bullet 6H_2O$, 97.0%, Kanto Chemical Co., Inc.). The TaON particles (2.0 g) were first suspended in Milli-Q water (~ 3 mL) containing the required amount of precursor (0.1 wt% unless stated, calculated as metal to the amount of TaON particles), and stirred using a glass rod in an evaporation dish in a hot water bath until complete dryness. Then, the dried samples were calcined at different temperatures ranging from 100 to 600 °C for 1 h in air. As for the loading of Ru species, ruthenium trichloride hydrate ($RuCl_3 \bullet nH_2O$, n = 1–3, 36–44% as Ru, Wako Pure Chemical Industries, Ltd.) was used as the precursor for impregnation and followed by heating at a fixed temperature of 200 °C for 1 h in air, since this procedure was confirmed to provide a highly uniform dispersion of $Ru(OH)_xCl_y$ species that exhibit the highest activity for IO_3^- reduction among those prepared at

varied temperatures.[21] The amount of the $Ru(OH)_xCl_y$ species was set to be 0.1 wt%, which was calculated as the metal Ru, unless stated. The loading of Co, Ir, and Rh species at temperatures range of 300–600 °C was carried out in advance of the $Ru(OH)_xCl_y$ loading to avoid the influence on the $Ru(OH)_xCl_y$ species loaded at 200 °C. Note that the $Ru(OH)_xCl_y$ species were preliminarily loaded when another component (Rh, Co or Ir species) was loaded at 100 °C. The samples co-loaded with two different cocatalysts will be denoted as Rh500-Ru200 (loaded with Rh species at 500 °C and subsequently with Ru species at 200 °C) for example, while those loaded with single cocatalyst will be denoted as Rh500 for example.

Characterization

Prepared samples were characterized by means of transmission electron microscopy (TEM, JEM-2100F, JEOL Ltd.) and X-ray photoelectron spectroscopy (XPS, MT-5500, Mg Kα, ULVAC-PHI, Inc.). Prior to the XPS measurements, a small amount of Au nanoparticles was sputtered onto each sample using magnetron sputtering (MSP-1S, Vacuum Device Inc.) for charge correction. The binding energy of the Au $4f_{7/2}$ peak was adjusted to 84.0 eV to correct the chemical shifts of the other elements.

Photocatalytic reactions

Photocatalytic oxidation of water (i.e., a half reaction of overall water splitting) was evaluated by using iodate anion (IO_3^-) as an electron acceptor in a Pyrex glass-made reaction vessel connected to a flow-type reaction system. Photocatalyst samples (50 mg) were suspended in 180 mL of Milli-Q water containing 1 mM of $NaIO_3$ (99.5%, Wako Pure Chemical Industries, Ltd.) by means of magnetic stirrer. Before each reaction, the dissolved gases (i.e., mainly O_2 and N_2) in suspension were thoroughly purged with Ar gas (99.999%). The suspension was irradiated by visible light (λ > 400 nm) using a Xe lamp (~ 360 mW cm^{-2}, output current 20 A, 300 W, LX-300F, Cermax) equipped with a cutoff filter (Hoya, L-42) and a cold mirror (Kenko, CM-1) under a constant flow of Ar (~ 20 mL min^{-1}). As for the two-step (i.e., overall) water splitting, another Pyrex glass-made reaction vessel connected to a closed gas circulation system was employed. Particles of zirconia-modified TaON were prepared according to a previous report[25] and used as a H_2-evolving photocatalyst after loading of Pt cocatalyst (denoted as $Pt/ZrO_2/TaON$). Both the $Pt/ZrO_2/TaON$ (50 mg) and one of the TaON sample (50 mg) were suspended together in 250 mL of Milli-Q water containing 0.5 mM of NaI (99.5%, Wako Pure Chemical Industries, Ltd.). Note that the reaction was initiated in the presence of an electron donor, i.e., iodide anion (I^-), alone. Then the suspension was thoroughly degassed by repeated evacuation of the gas phase by a vacuum pump, introduced by Ar gas (~ 50 torr), and finally exposed to the visible light. In both cases, the temperature of suspension was kept at 10 °C during the reaction by a flow of external circulating cooling water. Quantitative analysis of gases evolved was carried out using a gas chromatograph (GC-8A, Shimadzu,

thermal conductivity detector, Molecular Sieve 5A, Ar carrier). The apparent quantum yield (AQE) of O_2 evolution in half-reaction in the presence of IO_3^- (1 mM) at 420 nm was estimated by using monochromatic light obtained from a 300 W Xe lamp (~ 30 mW cm^{-2}, MAX-303, Asahi Spectra) fitted with a band-pass filter. The photon flux of the monochromatic light was measured by a silicon photodiode (Hioki 3664 optical power meter, Hioki E.E. Corporation).

Electrochemical measurements

To evaluate the catalytic activity of Rh species for water oxidation or IO_3^- reduction, the TaON particles loaded with Rh species were coated onto a conductive glass substrate (FTO, Asahi Glass Co., Ltd.) using a squeegee method as follows. Pastes of TaON-based sample were prepared by thoroughly mixing the TaON particles with a small amount of Milli-Q water by using a glass rod. The pastes prepared were spread onto an FTO substrate (4 cm × 1.5 cm, ~ 1 mg) and then dried in air at room temperature. The electrochemical cell used for the measurements consisted of a prepared electrode as the working electrode, a Ag/AgCl (3 M NaCl) as the reference electrode, a Pt wire as the counter electrode, and a sodium sulfate (Na_2SO_4, 99.0%, Wako Pure Chemical Industries, Ltd.) aqueous solution (0.1 M, 70 mL, pH 6 (without adjustment)) as the electrolyte. The dissolved gases in solution were thoroughly purged with Ar gas (99.999%) before each electrochemical measurement, and the applied potential of the working electrode was controlled using a potentiostat (VersaSTAT 3, Princeton Applied Research Co., Ltd.). The anodic photocurrent was investigated by linear sweep voltammetry or chronoamperometry measurement in the Na_2SO_4 aqueous solution under visible light irradiation using the 300 W Xe lamp equipped with the L-42 cutoff filter and CM-1 cold mirror (λ > 400 nm) to verify the electrocatalytic activity for water oxidation of the prepared electrodes. The onset potential of the cathodic current was investigated using linear sweep voltammetry in the Na_2SO_4 aqueous solution containing IO_3^- (1 mM) under dark conditions to estimate the overpotential for IO_3^- reduction on the prepared electrodes.

Results and discussion

Photocatalytic O_2 evolution on TaON loaded metal cation species in aqueous solution containing IO_3^- as an electron acceptor

The activity of cocatalyst-loaded TaON photocatalysts for water oxidation (i.e., O_2 evolution) was evaluated by the reaction in the presence of IO_3^- as the electron acceptor under visible light irradiation. The rates of O_2 evolution are plotted in Fig. 1(a) against the calcination temperatures at which the loading of Rh, Co, or Ir species was done. Note that all the TaON samples were loaded with $Ru(OH)_xCl_y$ via the calcination at 200 °C as a highly active cocatalyst for IO_3^- reduction.[24] Although the sole loading of $Ru(OH)_xCl_y$ species on TaON at 200 °C resulted in negligibly low rate of O_2 evolution (see Ru200 in Fig. S1), the co-loading of

Co species (at 100 °C) with $Ru(OH)_xCl_y$ significantly increased the rate of O_2 evolution from aqueous solution containing IO_3^- (see Ru200-Co100 in Fig. S1), as previously reported.[24] As seen in Fig. 1(a), the rates of O_2 evolution is significantly varied by the metal species co-loaded as well as the calcination temperature. As for the TaON loaded with Rh or Co species, the rates of O_2 evolution significantly increase with the increasing temperature up to 500 °C and drastically decrease at 600 °C. On the other hand, the calcination at 400 °C provided the highest rate among the Ir-loaded ones. The ratio of N/Ta at near surface of TaON particles calculated from the peak area of XPS spectra decreased from 0.6 to 0.3 after calcination at 500 °C and further to below 0.1 at 600 °C. Therefore, the deactivation of TaON surface (i.e., loss of nitrogen anions) is undoubtedly one of the main reasons for the significant decline in O_2 evolution rate at 600 °C independently of the metal species. One of the important findings here is that the co-loading of Rh species at relatively high temperature (e.g., 500 °C) with $Ru(OH)_xCl_y$ species resulted in obviously higher rate of O_2 evolution than the others.

Fig. 1(b) shows the representative time courses of O_2 evolution on samples co-loaded with two cocatalysts (Rh500-Ru200 and Ru200-Co100, included in Fig. 1(a)) along with those loaded with single cocatalyst (Rh500 and Ru300) for comparison. It has been reported that the RuO_2 species loaded on TaON at higher temperature than 250 °C work as a bi-functional cocatalyst, i.e., simultaneously enhancing reduction of IO_3^- and oxidation of water.[20, 24] Indeed, even the sole loading of Ru species at 300 °C triggers O_2 evolution (see Ru300), while the activity was lower than those co-loaded. The O_2 evolution rate on the Rh500-Ru200 sample is much higher than that on the Ru300 and also higher than that on the Ru200-Co100, which was demonstrated to exhibit the highest rate in our previous study,[24] indicating the superior performance of Rh species loaded at 500 °C. However, the sole loading of Rh species on TaON at 500 °C resulting in negligible activity (see Rh500), indicating that the Rh species loaded at 500 °C do not function as a bi-functional cocatalyst. These finding strongly suggested
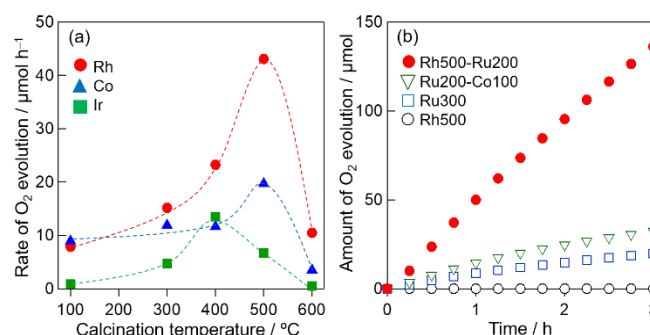

Figure 1. (a) The rate of O_2 evolution and (b) time courses of photocatalytic O_2 evolution on TaON photocatalyst co-loaded with metal cation (Rh, Co or Ir) species at different temperatures (100–600 °C) and Ru species at 200 °C from aqueous solution containing $NaIO_3$ (1 mM) under visible light irradiation (photocatalyst; 50 mg, amount of Milli-Q water; 180 mL, irradiation wavelength; λ > 400 nm).

that the Rh species loaded at 500 °C function as an effective water oxidation cocatalyst and therefore enhance O_2 evolution from IO_3^- aqueous solution with the help of the $Ru(OH)_xCl_y$.

Characterization of Rh species on TaON particles

The function of CoO_x and IrO_x species as the effective cocatalyst for photocatalytic or photoelectrochemical water oxidation have been well recognized and indeed employed in many systems.[26-32] For example, their loadings onto TaON photoanodes drastically enhance water oxidation, and thereby improve the stability against self-oxidative deactivation of TaON surface by holes.[26-28] On the other hand, the number of reports on enhanced water oxidation on Rh-related cocatalysts has been quite limited,[33, 34] while the electrocatalytic activity of Rh_2O_3 and RhO_2 has been demonstrated in some early works.[35, 36]

Fig. 2 shows XPS spectra of the TaON samples loaded with Rh-based cocatalyst alone via impregnation of $Na_3[RhCl_6] \cdot nH_2O$ and following calcination in air at different temperatures. The XPS spectra of commercial $Na_3[RhCl_6] \cdot nH_2O$, Rh_2O_3, $RhO_2 \cdot 2H_2O$, and Rh metal are also included for comparison. Note that a larger amount of Rh species (1.0 wt%) was loaded on each sample compared to the case of photocatalyst sample (0.1 wt%) to obtain XPS peaks with sufficiently high intensity and resolution. As shown in Fig. 2(a), the TaON samples loaded with Rh at or below 400 °C exhibit a $Rh3d_{5/2}$ main peak with a binding energy of approximately 309.8 eV, which is well consistent with that of the precursor $Na_3[RhCl_6] \cdot nH_2O$. In addition to the main peak, a weaker peak at ~ 307 eV is observed for the TaON loaded with Rh at 200, 300 or 400 °C. The position of later one is quite close to that of reference Rh metal, suggesting that these three samples contain Rh metal species to some extents. The $Rh3d_{5/2}$ peak of the Rh-loaded TaON sample prepared at 500 °C is obviously broadened and the peak top is observed at lower binding energy (~ 309.3 eV) compared to those prepared at or below 400 °C. The presence of residual Cl species is confirmed by the XPS spectra of Cl2p region for all the sample (see Fig. 2(b)), while the peak intensity is obviously decreased with increasing calcination temperature. The Cl/Rh ratios (determined by each area in XPS spectra) were estimated to be 4.5, 3.8 and 1.8 for the Rh-loaded TaON samples prepared at 100, 300 and 500 °C, respectively. This decrease of Cl species indicated the partial oxidation of $[RhCl_6]^{3-}$ precursor to some oxychloride species (e.g., RhO_xCl_y) via the calcination in air, while the peak position of $Rh3d_{5/2}$ was unchanged. Considering the deconvolution spectra of $Rh3d_{5/2}$ peak (see Fig. S2) and the Cl/Rh value (1.8), the Rh-loaded TaON sample prepared at 500 °C undoubtedly contains both partially oxidized precursor (i.e., RhO_xCl_y) and oxides (RhO_2 and Rh_2O_3). Although the ratio of such RhO_xCl_y species should be decreased by the increasing temperature, it was difficult to accurately estimate the ratio from the $Rh3d_{5/2}$ spectra. We noticed that the Cl/Rh ratio decreased after just stirring the samples in aqueous solution under dark condition for 3 h. For example, the Cl/Rh ratio

decreased from 3.8 to 1.5 for the sample prepared at 300 °C and from 1.8 to 0.9 for that prepared at 500 °C (see Fig. S3 for example). Such decrease in Cl/Rh ratio indicates that considerable fractions of the observed Cl content in XPS spectra were derived from the chloride anions or other related species that were physically adsorbed on the surface of TaON and/or RhO_xCl_y. Given the much smaller Cl/Rh value (0.9) obtained after stirring the sample compared to that of the precursor (~ 6), the majority of Rh species are undoubtedly oxide. As seen in Fig. 1(a), the rates of O_2 evolution on Rh-Ru co-loaded TaON samples drastically increased with increasing temperature of Rh loading. These findings strongly suggest that the Rh oxides (i.e., RhO_2 and Rh_2O_3 species, denoted as RhO_x) rather than the RhO_xCl_y species predominantly enhance the O_2 evolution when simultaneously loaded with the $Ru(OH)_xCl_y$ species, while one cannot exclude the minor role of RhO_xCl_y for enhancing O_2 evolution. The position of $Rh3d_{5/2}$ main peak of Rh500-Ru200 sample was almost unchanged (see Fig. S4) even after the photocatalytic reaction for 3 h with steady rate of O_2 evolution
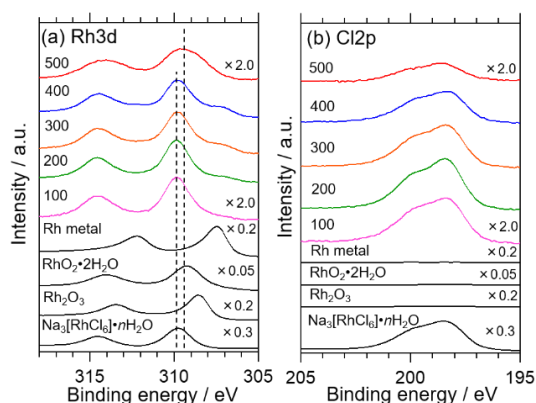

Figure 2. XPS spectra of (a) Rh3d region and (b) Cl2p region for TaON samples loaded with Rh species prepared at different calcination temperatures and those of reference samples. The binding energy of the deposited Au was adjusted to 84.0 eV.
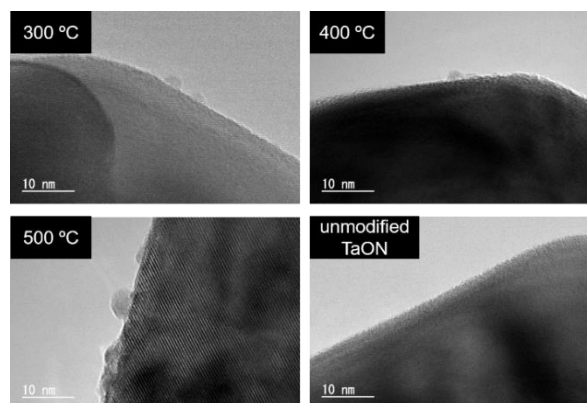

Figure 3. TEM images of 1.0 wt% Rh species loaded on TaON prepared at different calcination temperatures, along with that of unmodified TaON.

(see Fig. 1(b)), indicating that the Rh species (mainly RhO$_x$) loaded on Rh500-Ru200 sample can stably catalyze water oxidation during the reaction. The samples prepared with Rh(NO$_3$)$_3$•nH$_2$O precursor did not show the peak derived from the Rh metal species regardless of the calcination temperature (shown in Fig. S5). Therefore, the partial formation of Rh metal species is probably attributed to the specific nature of Na$_3$[RhCl$_6$]•nH$_2$O precursor, while the detailed mechanism has not yet be clarified. Note that, however, the activity of TaON samples loaded with Rh species from Rh(NO$_3$)$_3$•nH$_2$O, along with Ru species, were considerably lower compared to those prepared from Na$_3$[RhCl$_6$]•nH$_2$O. For example, the sample prepared from Rh(NO$_3$)$_3$•nH$_2$O exhibited the maximum O$_2$ evolution rate (19 μmol h^{-1}) via calcination at 300 °C as seen in Fig. S6, which is lower than that (43 μmol h^{-1}) obtained for the optimized sample loaded by Rh species from Na$_3$[RhCl$_6$]•nH$_2$O precursor.

Fig. 3 shows TEM images of the TaON samples loaded with Rh species (1.0 wt%) alone, along with that of unmodified TaON for comparison. Although the surface of unmodified TaON is basically smooth, some nanoparticles with diameters ranging from 2 to 5 nm are found on the surface of modified TaON samples; their particle size specifically increased with increasing temperature from 400 to 500 °C.

The role of Rh species loaded onto TaON particles

The evaluation of cocatalyst loaded on TaON for oxidative reaction (i.e., water oxidation) is almost impossible via direct electrochemical measurement due to the n-type nature of TaON (i.e., negligibly low concentration of holes in dark). The catalytic activity of Rh species loaded onto TaON was thus investigated by monitoring the anodic photocurrent in a Na$_2$SO$_4$ aqueous solution under visible light irradiation. In such n-type photoanode systems, the loading of effective cocatalyst for water oxidation is expected to increase photocurrent by enhancing the surface reaction (i.e., O$_2$ evolution) with photogenerated holes and thereby increasing the numbers of active electrons for photocurrent generation. Note that a larger amount of Rh species alone (1.0 wt%) compared to the case of photocatalyst (0.1 wt%) was loaded on the photoelectrode samples to make the difference in photocurrent more clearly. Each photoelectrode was prepared by spreading the Rh-loaded TaON particles onto an FTO substrate using a squeegee method without any calcination (just drying). Fig. 4(a) shows the photocurrent-potential relationship under chopped visible light irradiation for TaON photoelectrodes loaded with Rh species at different calcination temperatures (denoted as Rhx, x: calcination temperature in impregnation). The photocurrent generated on the Rh500 photoelectrode is obviously higher than that of unmodified one, while the enhancement in the photocurrent on Rh300 and Rh400 is unclear by the photocurrent-potential relationship. To clarify the role of Rh species, these photoelectrodes were subjected to continuous irradiation of visible light under a fixed potential of +1.2 V vs.

RHE. As seen in Fig. 4(b), the photocurrent on the unmodified TaON photoelectrode is immediately decreased just after the initiation of light irradiation and become almost zero within 20 min. This rapid decline is undoubtedly due to the occurrence of self-oxidative deactivation of the TaON surface, in which the photogenerated holes oxidize N^{3-} anions at the near surface of TaON (2N^{3-} + 6h$^+$ → N$_2$).[14] On the other hand, the Rh500 exhibits higher and steady photocurrent within 60 min, strongly suggesting that the Rh species loaded captured the considerable fraction of photogenerated holes and thereby suppressed the self-oxidative deactivation of TaON surface. The number of electrons passed through outer circuit during the photoelectrochemical reaction on Rh500 was estimated to be 0.38 μmol by the integration of photocurrent; this value is much larger than the molar amount of the Rh species loaded (~ 0.09 μmol). It can be therefore concluded that the observed photocurrent for Rh500 electrode was derived from water oxidation not from self-oxidation of the Rh species. These findings revealed that the Rh species loaded on TaON via the calcination at 500 °C, which mainly consist of RhO$_x$ species, function as effective cocatalyst for water oxidation in a similar manner to IrO$_x$ and CoO$_x$.[26-32] As for the Rh300 and Rh400, the photocurrents under continuous irradiation were slightly but obviously improved compared to unmodified one, strongly suggesting the catalytic activity of the Rh-related species loaded for water oxidation while their activity was undoubtedly lower compared to that loaded at 500 °C. Note that, the Rh500 electrode exhibits appreciable catalytic activity for IO$_3^-$ reduction but the activity is much lower compared to that of the Ru(OH)$_x$Cl$_y$ species as seen in Fig. S7. From these results it can be concluded that the high activity of Rh500-Ru200 sample for photocatalytic O$_2$ evolution from aqueous NaIO$_3$ solution is due to the simultaneous but independent promotion of water oxidation and IO$_3^-$ reduction by Rh and Ru species, respectively.
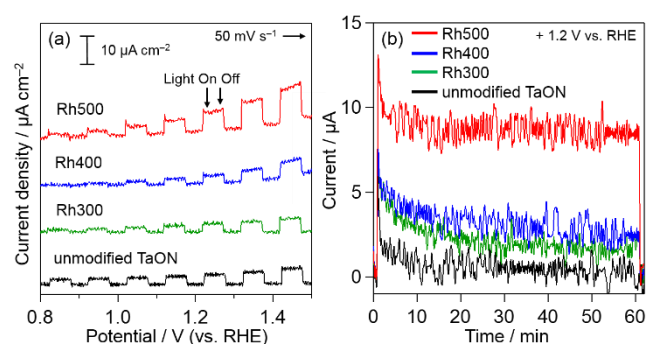

Figure 4. (a) Current–potential relationship and (b) time courses of photocurrent for Rh-loaded TaON electrode in Na$_2$SO$_4$ aqueous solution (0.1 M, pH 6) under visible light irradiation (λ > 400 nm).

Two-step water splitting reaction with IO_3^-/I^- redox mediator by combining Rh-loaded TaON as O_2-evolving photocatalyst with a H_2-evolving photocatalyst

To achieve overall water splitting (i.e., simultaneously generation of H_2 and O_2) via Z-scheme process, the photocatalysts employed should have sufficiently high selectivity for the forward reactions (i.e., reduction and oxidation of water) rather than the backward reactions (i.e., unfavorable reduction and oxidation of redox species). In the present case, the TaON-based photocatalyst, applied to O_2-evolving part, must have the capability of oxidizing water to O_2 even in the presence of considerable amount of I^- in the solution.[37] Because the oxidation of I^- is thermodynamically favorable than the oxidation of water, backward reaction, i.e., oxidation of I^- ($I^- + 3H_2O + 6h^+ \longrightarrow IO_3^- + 6H^+$), readily occurs and suppresses the O_2 evolution unless the photocatalyst possesses sufficiently high selectivity toward water oxidation. To evaluate the selectivity toward water oxidation, the photocatalytic O_2 evolution was carried out in the coexistence of IO_3^- and I^-. Fig. 5(a) shows representative time courses of O_2 evolution for Rh500-Ru200, Ru200-Co100 and Ru300 sample from aqueous solution containing both $NaIO_3$ (1 mM) and NaI (0.2 mM). The Rh500-Ru200 sample generates O_2 with steady rate even in the co-presence of IO_3^- and I^-, while the rate is obviously lower than that observed in the presence of IO_3^- alone (see Fig. 1(b)) undoubtedly due to the occurrence of backward reaction (i.e., oxidation of I^-) to some extent. Importantly, the present Rh500-Ru200 photocatalyst afforded much higher O_2 evolution rate compared to those previously reported Ru200-Co100 and Ru300 (loaded with the bi-functional RuO_2).[20, 24] Fig. 5(b) summarizes the rates of O_2 evolution on the TaON samples loaded with two cocatalysts from aqueous solution containing both IO_3^- and I^-. A comparison between Fig. 1(a) and Fig. 5(b) reveals that the rates were fallen by approximately 40-50% by the coexistence of I^- undoubtedly due to the occurrence of backward reaction. The similar trends observed between Fig. 1(a) and Fig. 5(b), except for the absolute rates, imply that the
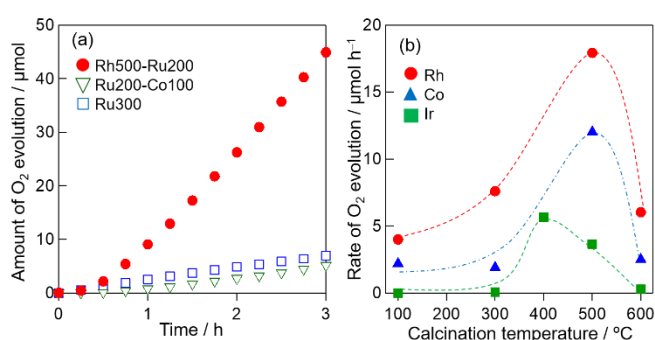
majority of backward reaction (oxidation of I^-) occurs on the naked surface of TaON rather than the surface of cocatalysts in the present reaction condition.

Finally, the Z-scheme water splitting system was constructed by combining the Rh500-Ru200 sample as the O_2-evolving photocatalyst and a $Pt/ZrO_2/TaON$ sample as the H_2-evolving photocatalyst in the presence of IO_3^-/I^- redox mediator under visible light irradiation. The loading amounts of Rh and Ru species for Rh500-Ru200 are set at 0.05 and 0.1 wt%, respectively, which were determined as the optimum amounts based on the results shown in Fig. S8 and S9. The apparent quantum yield (AQE) for O_2 evolution over Rh500-Ru200 sample in half-reaction in the presence of IO_3^- was determined to be ~ 6.9% at 420 nm. As shown in Fig. 6, the H_2 and O_2 are produced steady rate in a 2:1 stoichiometric ratio by using the Rh500-Ru200 sample as O_2-evolving photocatalyst; the evolution rates of the Rh500-Ru200 are obviously higher compared to that of the Ru200-Co100 and Ru300 sample. The total amount of H_2 gas evolved during 16 h of photoirradiation reached ~ 250 µmol, which is substantially larger than the amount of NaI employed as the shuttle redox mediator (125 µmol) for the reaction, indicating that the overall water splitting proceeded photocatalytically via the redox cycle between IO_3^- and I^-. On the other hand, the amount of evolved O_2 in the combination of Ru300 or Ru200-Co100 sample with $Pt/ZrO_2/TaON$ is smaller than the stoichiometric value estimated from the amount of evolved H_2. Note that the reactions were initiated in the presence of electron donor I^- alone (0.5 mM). Thus, the reduction of water to H_2 and oxidation of I^- to IO_3^- should be occurred on the $Pt/ZrO_2/TaON$ photocatalyst in the initial period. However, as revealed by the results shown in Fig. 5(a), the activity of Ru300 and Ru200-Co100 for O_2 evolution in the co-existence of IO_3^- and I^- is lower than that of Rh500-Ru200, resulting in the deviation of O_2 generation from H_2 evolution and also the accumulation of IO_3^- in the solution. In the case of

Figure 5. (a) Time courses of photocatalytic oxidation of water and (b) the rate of O_2 evolution on TaON photocatalyst co-loaded with metal cation (Rh, Co or Ir) species at different temperatures (100–600 °C) and Ru species at 200 °C from aqueous solution containing $NaIO_3$ (1 mM) with NaI (0.2 mM) under visible light irradiation (photocatalyst; 50 mg, amount of Milli-Q water; 180 mL, irradiation wavelength; λ > 400 nm).
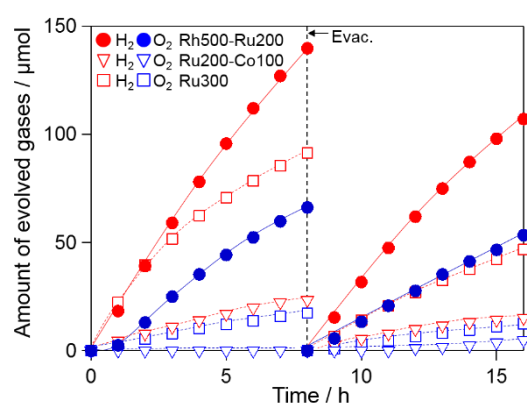

Figure 6. Time courses of photocatalytic evolution of H_2 and O_2 using a mixture of 0.5 wt%$Pt/ZrO_2/TaON$ photocatalyst (50 mg) and Rh500-Ru200, Ru200-Co100 or Ru300 photocatalyst (50 mg) suspended in an aqueous solution containing NaI (0.5 mM) under visible light irradiation (Milli-Q water; 250 mL, irradiation wavelength; λ > 400 nm).

Ru200-Co100, not only O_2 evolution but also H_2 evolution was suppressed. It appears that the Co-based cocatalyst (Co100) selectively oxidize I^-, instead of water, in the present condition (note that the concentration of NaI is higher than the case of half reactions shown in Fig. 5(a)), resulting in the accumulation of IO_3^- from both H_2- and O_2-evolving photocatalysts. Such accumulation of IO_3^- undoubtedly cause the backward reaction on H_2-evolving photocatalyst (i.e., the reduction of IO_3^- instead of water) and consequently decrease the rate of H_2 evolution. These results demonstrated that the use of independently-optimized dual-cocatalysts for each reaction is effective for improving the total efficiency in Z-scheme water splitting with IO_3^-/I^- redox, in the same manner as the previous reported dual cocatalysts for one-step water splitting.[38]

Conclusion

In summary, this study demonstrated that RhO_x species loaded on TaON at the high temperature of 500 °C function as a highly efficient cocatalyst for water oxidation and thus significantly increase the rate of O_2 evolution from an aqueous solution containing IO_3^- electron acceptor with the help of previously-found $Ru(OH)_xCl_y$ cocatalyst. Consequently, the TaON sample co-loaded with RhO_x at 500 °C and $Ru(OH)_xCl_y$ at 200 °C exhibited about 5 times higher rate of O_2 evolution from IO_3^- aqueous solution under visible light irradiation compared to the previously ones including the TaON loaded with a bi-functional RuO_2 cocatalyst. Importantly, the superiority of the co-loaded sample became more prominent when the photocatalytic reaction was carried out in the co-existence of IO_3^- and I^-, in which about 10 times higher O_2 evolution rate was obtained, strongly suggested that the RhO_x species can selectively promote the water oxidation rather than unfavorable backward reaction, i.e., oxidation of I^-. Thus, the total efficiency of the Z-scheme system was significantly improved by using of the TaON photocatalyst co-loaded with the Rh and Ru species as the O_2-evolving photocatalyst, in place of the TaON loaded with conventional RuO_2 alone. The findings in the present study will offer useful insights into the designing of highly efficient photocatalysts, not only the presence oxynitirides, for Z-scheme type water splitting with a redox couple such as IO_3^-/I^- by employing the independently-optimized cocatalysts for favorable oxidation and reduction, respectively, and thereby provide the possibility of highly efficient water splitting under solar light based on two-step excitation mechanism in a similar manner to the natural photosynthesis.

Conflicts of interest

There are no conflicts to declare.

Acknowledgements

References

1   A. Fujishima and K. Honda, *Nature*, 1972, **238**, 37.
2   K. Domen, S. Naito, M. Soma, T. Onishi and K. Tamaru, *J. Chem. Soc., Chem. Commun.*, 1980, 543.
3   K. Maeda, T. Takata, M. Hara, N. Saito, N. Inoue, H. Kobayashi and K. Domen, *J. Am. Chem. Soc.*, 2005, **127**, 8286.
4   K. Sayama, K. Mukasa, R. Abe and H. Arakawa, *Chem. Commun.*, 2001, 2416.
5   A. Kudo and Y. Miseki, *Chem. Soc. Rev.*, 2009, **38**, 253.
6   R. Abe, *Bull. Chem. Soc. Jpn.*, 2011, **84**, 1000.
7   Y. Wang, H. Suzuki, J. Xie, O. Tomita, D. J. Martin, M. Higashi, D. Kong, R. Abe and J. Tang, *Chem. Rev.*, 2018, **118**, 5201.
8   K. Sayama, K. Mukasa, R. Abe, Y. Abe and H. Arakawa, *J. Photochem. Photobiol. A*, 2002, **148**, 71.
9   H. Kato, M. Hori, R. Konta, Y. Shimodaira and A. Kudo, *Chem. Lett.*, 2004, **33**, 1348.
10 R. Abe, T. Takata, H. Sugihara and K. Domen, *Chem. Commun.*, 2005, 3829.
11 Y. Sasaki, H. Kato and A. Kudo, *J. Am. Chem. Soc.*, 2013, **135**, 5441.
12 Y. Miseki, S. Fujiyoshi, T. Gunji and K. Sayama, *J. Phys. Chem. C*, 2017, **121**, 9691.
13 K.Tsuji, O. Tomita, M. Higashi and R. Abe, *ChemSusChem*, 2016, **9**, 2201.
14 G. Hitoki, A. Ishikawa, T. Takata, J. N. Kondo, M. Hara and K. Domen, *Chem. Lett.*, 2002, **31**, 736.
15 W. A. Chun, A. Ishikawa, H. Fujishima, T. Takata, J. N. Kondo, M. Hara, M. Kawai, Y. Matsumoto and K. Domen, *J. Phys. Chem. B*, 2003, **107**, 1798.
16 D. Yamashita, T. Takata, M. Hara, J. N. Kondo and K. Domen, *Solid State Ionics*, 2004, **172**, 591.
17 S. Chen, Y. Qi, T. Hisatomi, Q. Ding, T. Asai, Z. Li, S. S. K. Ma, F. Zhang, K. Domen and C. Li, *Angew. Chem. Int. Ed.*, 2015, **54**, 8498.
18 Y. Qi, S. Chen, M. Li, Q. Ding, Z. Li, J. Cui, B. Dong, F. Zhang and C. Li, *Chem. Sci.*, 2017, **8**, 437.
19 M. Higashi, R. Abe, A. Ishikawa, T. Takata, B. Ohtani and K. Domen, *Chem. Lett.*, 2008, **37**, 138.
20 K. Maeda, R. Abe and K. Domen, *J. Phys. Chem. C*, 2011, **115**, 3057.
21 M. Tabata, K. Maeda, M. Higashi, D. Lu, T. Takata, R. Abe and K. Domen, *Langmuir*, 2010, **26**, 9161.
22 R. Abe, M. Higashi and K. Domen, *ChemSusChem.*, 2011, **4**, 228.
23 H. Suzuki, O. Tomita, M. Higashi and R. Abe, *Catal. Sci. Technol.*, 2015, **5**, 2640.
24 Y. Iwase, O. Tomita, M. Higashi and Ryu Abe, *Sustainable Energy Fuels*, 2017, **1**, 748.
25 K. Maeda, H. Terashima, K. Kase, M. Higashi, M. Tabata and K. Domen, *Bull. Chem. Soc. Jpn.*, 2008, **81**, 927.
26 R. Abe, M. Higashi and K. Domen, *J. Am. Chem. Soc.*, 2010, **132**, 11828.
27 M. Higashi, K. Domen and R. Abe, *Energy Environ Sci.*, 2011, **4**, 4138.
28 M. Higashi, K. Domen and R. Abe, *J. Am. Chem. Soc.*, 2012, **134**, 6968.
29 K. Maeda, D. Lu and K. Domen, *Ang. Chem., Int. Ed.*, 2013, **52**, 6488.
30 X. Deng and H. Tüysüz, *ACS Catal.*, 2014, **4**, 3701.

31 A. Xiong, T. Yoshinaga, T. Ikeda, M. Takashima, T. Hisatomi, K. Maeda, T. Setoyama, T. Teranishi and K. Domen, *Eur. J. Inorg. Chem.*, 2014, **4**, 767.
32 S. Chen, S. Shen, G. Liu, Y. Qi, F. Zhang and C. Li, *Angew. Chem.*, 2015, **127**, 3090.
33 W. Luo, Z. Yang, Z. Li, J. Zhang, J. Liu, Z. Zhao and Z. Wang, *Energy Environ. Sci.*, 2011, **4**, 4046.
34 W. Chen, H. Wang, L. Mao, X. Chen and W. Shangguan, *Catal. Commun.*, 2014, **57**, 115.
35 A. Harriman, I. J. Pickering, J. M. Thomas and P. A. Christensen, *J. Chem. SOC., Faraday Trans. I*, 1988, **84**, 2795.
36 A. Mills and T. Russell, *J. Chem. Soc. Faraday Trans.*, 1991, **87**, 1245.
37 R. Abe, K. Sayama and H. Sugihara, *J. Phys. Chem. B*, 2005, **109**, 16052.
38 K. Maeda, A. Xiong, T. Yoshinaga, T. Ikeda, N. Sakamoto, T. Hisatomi, M. Takashima, D. Lu, M. Kanehara, T. Setoyama, T. Teranishi and K. Domen, *Angew. Chem. Int. Ed*. 2010, **49**, 4096.

254x190mm (96 x 96 DPI)